Exp. Theo. NANOTECHNOLOGY 10 (2026) 257-275 https://doi.org/10.56053/10.S.257

Purification, characterization and antibacterial potential of streptococcus-derived protease: Insights into biomedical applications

Hajer Sabah Shabram[*], *Entesar Hussain Ali*

Applied Sciences Department, University of Technology- Iraq, Baghdad 10066, Iraq
[*]) Email: hajersabah25@gmail.com

Received 17/11/2025, *Received in revised form* 15/12/2025, *Accepted* 28/12/2025, *Published* 15/2/2026

Proteases are key industrial enzymes with significant biomedical potential. A protease-producing *Streptococcus* isolate is cultivated in casein–starch medium under optimized conditions (pH 7.4, 37 °C, 36 h). The enzyme is purified by ammonium sulfate precipitation, dialysis, ion exchange, and gel filtration, yielding a 2.74-fold increase in specific activity (13.8 to 37.83 U/mg) with 4.2% final yield. SDS-PAGE confirmed near-homogeneity. The protease showed optimum activity at 40 °C and pH 7.0, with moderate thermostability. Accordingly, the present study aims to isolate and identify a protease-producing *Streptococcus* strain, purify the extracellular enzyme through a multistep process, and characterize its biochemical properties in terms of activity, stability, and optimal operating conditions. Furthermore, the antibacterial potential of the purified protease is evaluated against both Gram-positive (*Staphylococcus aureus*) and Gram-negative (*Escherichia coli*) bacteria to assess its efficacy as a natural antimicrobial agent. Through this investigation, the work seeks to establish the *Streptococcus*-derived protease as a promising candidate for biomedical and therapeutic applications, particularly in the context of enzyme-based antibacterial strategies. Antibacterial assays revealed dose-dependent inhibition of *Escherichia coli* and *Staphylococcus aureus*, with stronger activity against Gram-positive bacteria, highlighting its potential as a promising antimicrobial biocatalyst.

Keywords: Streptococcus-derived enzyme; Purification; Antibacterial.

1. INTRODUCTION

Nanotechnology has revolutionized biomedical research by enabling precise manipulation of materials at the molecular and atomic levels [1]. Nanoparticles exhibit unique physicochemical properties, including high surface-to-volume ratios, tunable surface chemistry, and enhanced reactivity, making them suitable for therapeutic and diagnostic applications [2]. In medicine, nanomaterials are widely applied in targeted drug delivery, antimicrobial coatings, biosensing, and regenerative tissue engineering [3]. Their ability to cross biological barriers and interact with cellular components enhances efficacy while minimizing side effects [4]. Integration of nanotechnology with enzyme-based systems further expands potential biomedical applications, particularly in combating antibiotic resistance and improving therapeutic precision [5]. Proteases are one of the most important classes of industrial enzymes, accounting for nearly 60% of the global enzyme market due to their versatile catalytic properties [6]. They are widely employed in pharmaceutical, food, detergent, and leather industries, as well as in environmental and biomedical applications [7]. Microbial proteases are particularly attractive because of their cost-effective large-scale production, high catalytic efficiency, and ability to function under diverse physicochemical conditions [8]. Among microbial sources, Streptococcus species have recently gained attention due to their potential to produce extracellular proteases with unique structural and functional properties [9]. The biochemical significance of proteases lies in their ability to hydrolyze peptide bonds, releasing amino acids and bioactive peptides that can exert nutritional, functional, or therapeutic benefits. In addition to their industrial utility, proteases have been increasingly recognized for their biomedical relevance, particularly as antimicrobial and antioxidant agents [10]. The emergence of antibiotic resistance has renewed interest in enzyme-based antibacterial strategies, where proteases can destabilize microbial cell walls, degrade essential proteins, and potentiate the activity of conventional antibiotics [11]. Purification and characterization of microbial proteases are essential to understanding their catalytic properties, stability, and potential applications [12]. Traditional purification strategies, including ammonium sulfate precipitation, dialysis, ion-exchange chromatography, and gel filtration, allow progressive enrichment of the target enzyme while monitoring specific activity, yield, and stability [13]. Complementary biochemical assays, such as SDS-PAGE, provide insights into molecular weight and purity, whereas functional assays evaluate activity under varying pH, temperature, and incubation conditions [14]. In addition to antibacterial potential, the antioxidant activity of microbial proteases has drawn significant attention [15]. Radical scavenging properties of protease hydrolysates contribute to cellular protection against oxidative stress, further highlighting their biomedical promise [16]. The integration of enzyme technology with nanotechnology provides an advanced platform to enhance enzyme stability, broaden antibacterial spectra, and deliver therapeutic proteases in targeted applications [17-19]. This paper describes the production, purification, and antibacterial evaluation of a protease derived from a *Streptococcus* isolate. The enzyme is purified using ammonium sulfate precipitation, dialysis, ion-exchange, and gel filtration, achieving increased specific activity with near-homogeneous purity confirmed by SDS-PAGE. Antibacterial assays revealed dose-dependent inhibition against *Escherichia coli* and *Staphylococcus aureus*, with stronger activity observed against the Gram-positive strain. These findings demonstrate the potential of *Streptococcus*-derived protease as a promising antibacterial agent, highlighting its value for biomedical applications and its possible role as an alternative or adjunct to conventional antibiotic therapies.

2. MATERIALS AND METHODS

2.1 Materials and equipment

A *Streptococcus* isolate is employed for protease production. The culture medium contained casein, starch, KH_2PO_4, KNO_3, NaCl, $MgSO_4 \cdot 7H_2O$, $CaCO_3$, and $FeSO_4 \cdot 7H_2O$, nanoparticles (NPs) all of analytical grade. Chemicals and reagents included Tris-HCl, Na_2CO_3, sodium potassium tartrate, $CuSO_4$, Folin–Ciocalteu reagent, ammonium sulfate, sodium bicarbonate, sodium acetate, bovine serum albumin (BSA), Coomassie Brilliant Blue, 2,2-diphenyl-1-picrylhydrazyl (DPPH), resazurin dye, and crystal violet. L-tyrosine and BSA served as standards for activity and protein quantification. Chromatography resins included DEAE–Cellulose (ion-exchange) and Sephadex G-100 (gel filtration). Mueller–Hinton agar (MHA) and nutrient broth are used for antibacterial testing. Equipment included a shaking incubator, refrigerated centrifuge, spectrophotometer, microplate reader, electrophoresis system, dialysis tubing (10,000 MW cut-off), and sterile 96-well microtiter plates.

2.2 Methods

Enzyme production is carried out by cultivating the *Streptococcus* isolate in optimized medium. The pH is adjusted to 7.4, and fermentation proceeded at 37 °C for 36 h at 200 rpm. The culture broth is centrifuged (10,000 rpm, 15 min, 4 °C), and the supernatant is collected as crude enzyme extract [20-22]. Enzyme activity assay is performed using casein as the substrate. One milliliter of enzyme is incubated with 2% casein in Tris-HCl buffer (pH 8.5) at 30 °C for 10 min. The reaction is terminated with trichloroacetic acid (TCA) and centrifuged. The supernatant is neutralized with sodium carbonate and reacted with Folin–Ciocalteu reagent. Absorbance is measured at 660 nm, and activity is expressed using an L-tyrosine standard curve. One unit (U) of activity is defined as [23-25]:

$$1\,U = \frac{\mu g\ tyrosine\ released}{mL \times min} \tag{1}$$

Protein concentration is quantified using the Lowry method. A standard curve is constructed with BSA (0–100 μg/mL). Absorbance at 600 nm is plotted against concentration, and protein content in unknown samples is calculated by interpolation. Purification of enzyme is conducted in sequential steps. Crude extract is precipitated with ammonium sulfate (20–80% saturation) and centrifuged. The pellet is dissolved in phosphate buffer and subjected to dialysis (10,000 MW cut-off) for 24 h. The dialyzed sample is loaded onto a DEAE–Cellulose ion-exchange column and eluted with a linear NaCl gradient (0–1 M). Active fractions are pooled, concentrated, and further purified by Sephadex G-100 gel filtration. Fractions are analyzed at 280 nm, and activity is measured. Characterization of protease included determination of optimum temperature (25–55 °C), thermal stability (incubation for 30 min followed by residual activity), optimum pH (pH 4–9), and pH stability (30 min pre-incubation at 35 °C in respective buffers). Time-course studies (12–48 h) are also performed to identify peak enzyme production. SDS-PAGE is used to analyze enzyme purity. Samples are denatured, loaded on 15% resolving and 5% stacking gels, electrophoresed in Tris–glycine buffer, and stained with Coomassie Brilliant Blue. Antibacterial activity is tested against *Escherichia coli* and *Staphylococcus aureus* by the agar well diffusion method. Inhibition zones are measured in millimetres after incubation at 37 °C for 24 h.

3. RESULTS AND DISCUSSION

3.1 Enzyme production and activity

Protease production by *Streptococcus* is successfully achieved in casein–starch medium under optimized fermentation conditions. After 36 h of incubation at 37 °C with shaking at 200 rpm, the culture supernatant obtained by centrifugation represented the crude enzyme extract. The yield of crude enzyme is 400 mL, with an initial activity of 36.7 U/mL and a protein concentration of 2.66 mg/mL, corresponding to a specific activity of 13.8 U/mg protein. These values established the baseline for subsequent purification steps. To quantify enzyme activity, a standard calibration curve is constructed using L-tyrosine as the reference compound. The release of tyrosine equivalents upon casein hydrolysis is measured spectrophotometrically at 660 nm, and a linear relationship is observed between absorbance and concentration (Fig. 1). The slope of this curve is used to calculate enzyme activity in all subsequent assays.

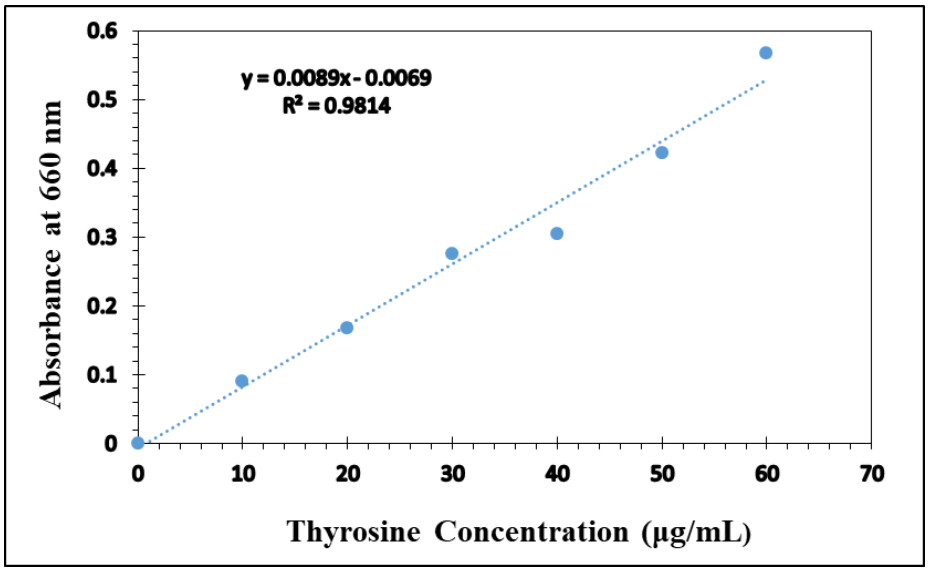

Figure 1 Standard calibration curve of L-tyrosine for protease activity.

Similarly, protein concentration is determined by the Lowry method using bovine serum albumin (BSA) as the standard. Serial dilutions of BSA ranging from 0–100 µg/mL are prepared (Table 1) which presents the serial dilutions of BSA used to generate the protein calibration curve. The final concentrations ranging from 0–100 µg/mL provided a reliable standard for protein estimation in enzyme samples. The calibration curve demonstrated a strong linearity between absorbance at 600 nm and BSA concentration (Fig. 2), confirming the reliability of the method for accurate protein quantification in crude and purified enzyme samples.

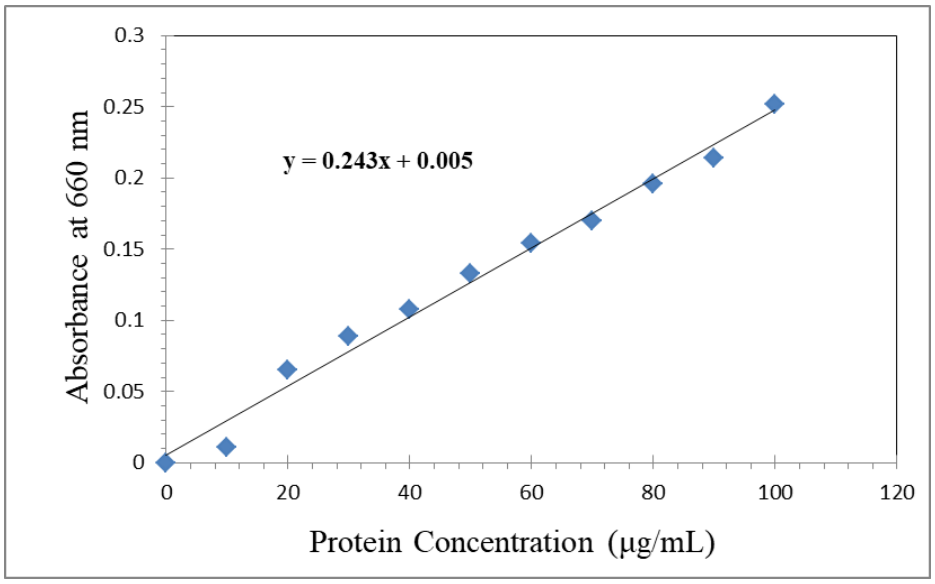

Figure 2 Standard calibration curve of bovine serum albumin (BSA) for protein estimation.

Time-course monitoring revealed that protease production increased steadily from 12 to 36 h, reaching a maximum at 36 h of incubation, after which activity plateaued. This indicates that the enzyme is produced predominantly during the late exponential to early stationary growth phases, consistent with secondary metabolite secretion in many bacteria.

Table 1 Preparation of bovine serum albumin (BSA) concentrations from stock solution (100 µg/mL) used as standard for protein estimation.

Tube No.	Volume of BSA (mL)	Volume of DW (mL)	Final volume (mL)	Final concentration (µg/mL)
1	0.0	1.0	1.0	0
2	0.1	0.9	1.0	10
3	0.2	0.8	1.0	20
4	0.3	0.7	1.0	30
5	0.4	0.6	1.0	40
6	0.5	0.5	1.0	50
7	0.6	0.4	1.0	60
8	0.7	0.3	1.0	70
9	0.8	0.2	1.0	80
10	0.9	0.1	1.0	90
11	1.0	0.0	1.0	100

3.2 Enzyme purification

The *Streptococcus*-derived protease is purified in a sequential process involving ammonium sulphate precipitation, dialysis, ion-exchange chromatography, and gel filtration chromatography. The overall purification profile is summarized in Table 2.

Table 2 Stepwise purification profile of protease derived from Streptococcus. The table summarizes changes in enzyme activity, protein concentration, specific activity, purification fold, and yield (%) across successive purification steps.

Purification Step	Volume (mL)	Enzyme Activity (U/mL)	Protein Concentration (mg/mL)	Specific Activity (U/mg)	Total Activity (U)	Purification Fold	Yield (%)
Crude Enzyme	400	36.7	2.66	13.8	14,680	1.0	100
Ammonium Sulfate Precipitation (80%)	35	52.6	1.98	26.57	1,842	1.93	12.5
Dialysis + Sucrose Concentration	25	46.4	1.66	27.95	1,160	2.03	7.9
Ion Exchange Chromatography (DEAE–Cellulose)	15	47.7	1.44	33.13	715.5	2.40	4.9
Gel Filtration Chromatography (Sephadex G-100)	15	45.4	1.20	37.83	618	2.74	4.2

In the first step, ammonium sulfate precipitation (80% saturation) concentrated the crude extract from 400 mL to 35 mL, resulting in an increase in enzyme activity from 36.7 U/mL in the crude enzyme to 52.6 U/mL. The protein concentration decreased from 2.66 to 1.98 mg/mL, which led to an improvement in specific activity from 13.8 to 26.57 U/mg, corresponding to a 1.93-fold purification. However, the total activity dropped sharply to 1842 U, giving a yield of only 12.5%. These results are illustrated in the precipitation profile shown in Fig. 3, where the protease-rich precipitate is separated from non-protein impurities.

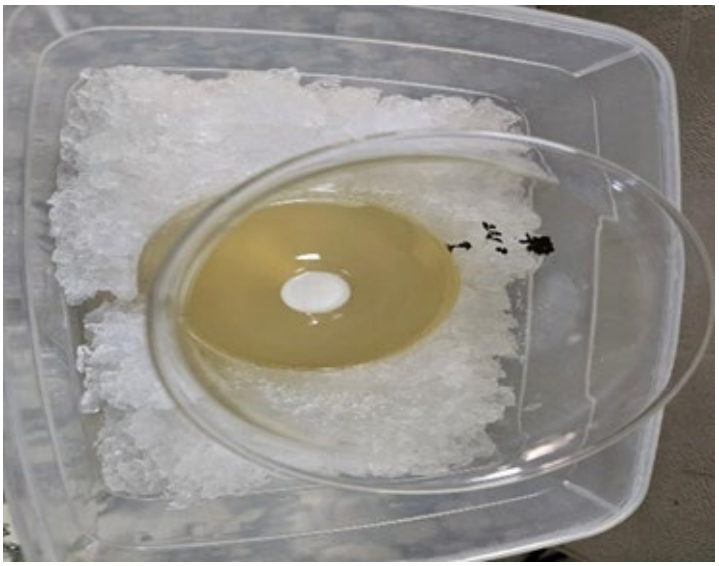

Figure 3 Ammonium sulphate precipitation profile. → Confirms enrichment of enzyme in the precipitate.

Subsequent dialysis and sucrose concentration removed residual salts and low-molecular-weight contaminants, reducing protein concentration to 1.66 mg/mL while maintaining enzyme activity at 46.4 U/mL. This yielded a specific activity of 27.95 U/mg, representing a 2.03-fold purification relative to the crude extract. The total activity decreased further to 1160 U, with a yield of 7.9% (Table

2). The third step, ion-exchange chromatography on DEAE–Cellulose, selectively separated proteins based on their charge. As shown in the chromatogram (Fig. 5), protease activity is associated with a distinct elution peak obtained at moderate NaCl concentrations. Fractions corresponding to this peak exhibited enzyme activity of 47.7 U/mL at a protein concentration of 1.44 mg/mL, resulting in a specific activity of 33.13 U/mg and a 2.4-fold purification (Table 2). The SDS-PAGE analysis of ion-exchange fractions (Fig. 6) confirmed a reduction in contaminating protein bands and enrichment of the protease band at its expected molecular weight.

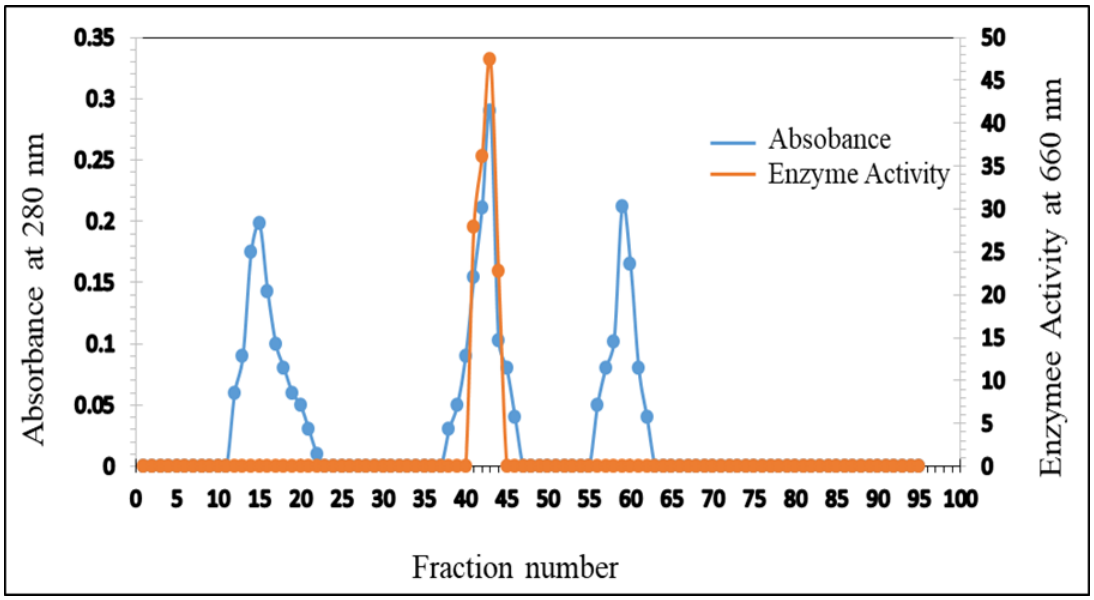

Figure 5 Ion-exchange chromatogram. → Shows selective elution of protease fractions.

Figure 6 SDS-PAGE after ion exchange. → Confirms reduction in contaminating proteins.

Finally, gel filtration chromatography on Sephadex G-100 provided size-based separation, producing a well-defined elution profile with a single major peak (Fig. 7). The active fractions demonstrated activity of 45.4 U/mL with protein concentration reduced to 1.20 mg/mL, yielding the highest specific activity of 37.83 U/mg. This corresponded to a 2.74-fold purification compared with the crude extract, though the final total activity is only 618 U, reflecting a yield of 4.2% (Table 2). The final SDS-PAGE profile (Fig. 8) revealed a single prominent band, confirming that the protease is purified to near homogeneity.

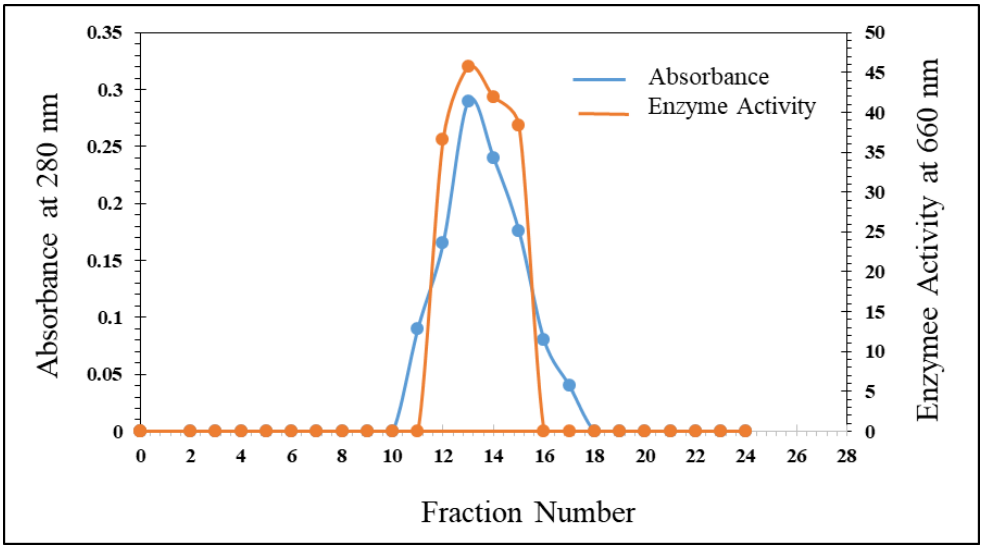

Figure 7 Gel filtration chromatogram. → Illustrates separation by molecular size and enrichment of active fractions.

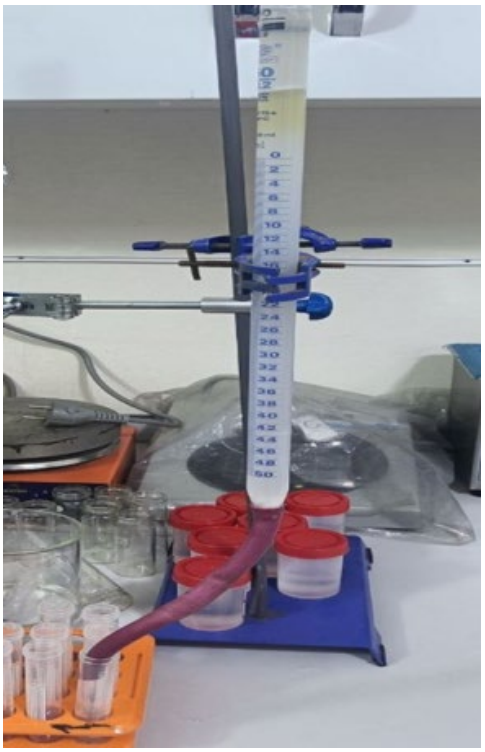

Figure 8 SDS-PAGE of final enzyme. → Shows a single sharp band confirming purity.

Together, these results demonstrate that sequential purification steps progressively increased the protease's specific activity from 13.8 to 37.83 U/mg (Table 2), reflecting removal of contaminating proteins. However, purification is accompanied by progressive losses in total yield, a typical trade-off in protein purification workflows.

3.3 Enzyme characterization

The biochemical properties of the purified *Streptococcus* protease are characterized in relation to optimum temperature, thermal stability, optimum pH, pH stability, and production time course. These findings are supported by Figs. 9–15, each providing a graphical representation of the enzyme's functional performance.

3.3.1 Optimum temperature

The effect of temperature on enzyme activity is examined between 25–55 °C. As shown in Fig. 9, protease activity increased gradually with temperature and reached a maximum at 40 °C. At higher temperatures, activity decreased, with a sharp decline at 50–55 °C. This optimum is further validated in Fig. 10, which confirmed maximum activity at 40 °C followed by a steep reduction beyond 45 °C. Together, Figs. 9 and 10 confirm the mesophilic nature of the protease, consistent with physiological temperature ranges.

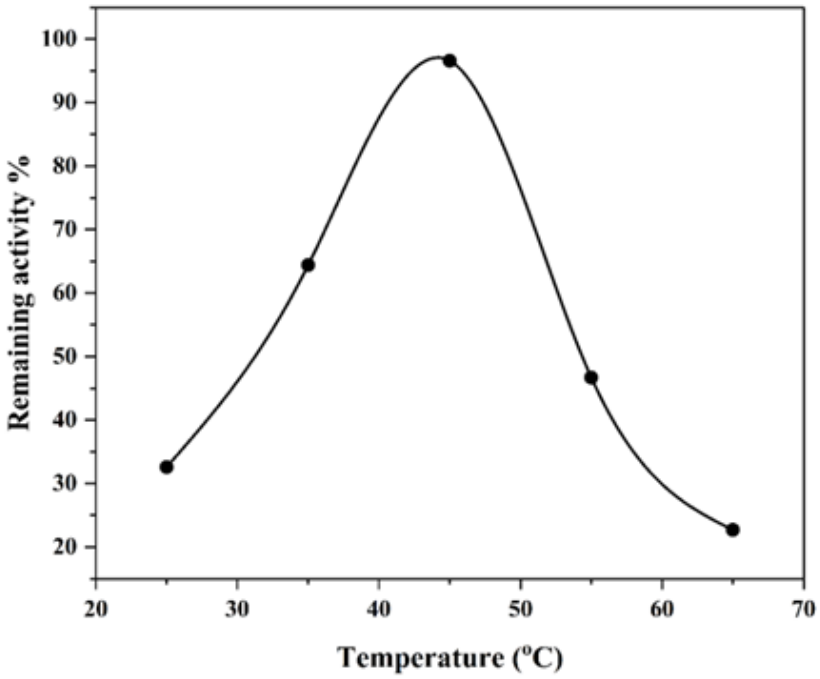

Figure 9 Effect of temperature on protease activity.

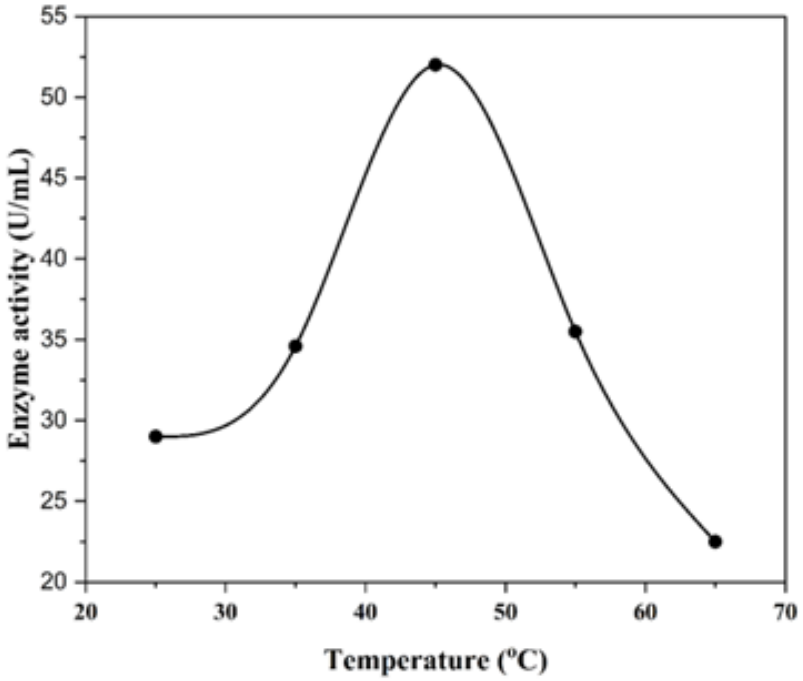

m.

3.3.2 Optimum pH

The effect of pH on protease activity is determined using buffers ranging from pH 4.0 to 9.0. As shown in Fig. 11, enzyme activity increased gradually from acidic conditions and reached a maximum at pH 7.0, after which it declined sharply at alkaline pH. This profile indicates that the protease is most active under near-neutral conditions, which aligns with physiological pH values and enhances its potential for biomedical use. Similar findings have been reported for microbial proteases with optimum activity between pH 6.5–8.0 [1].

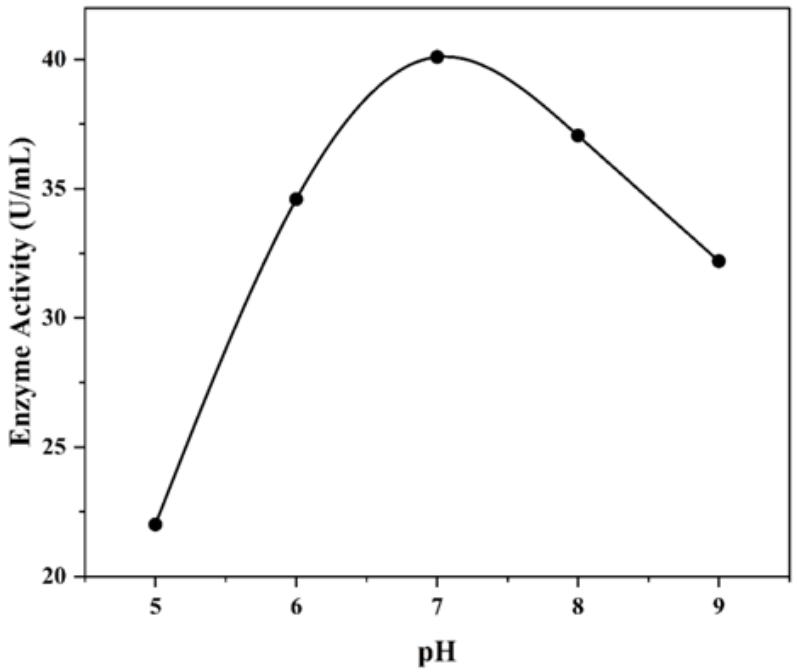

Figure 11 Effect of pH on protease activity.

3.3.3 PH stability

Protease activity is also measured across a pH range of 4.0–9.0. The enzyme displayed increasing activity from acidic to neutral conditions, with maximum activity at pH 7.0. This is demonstrated in Fig. 11 and further confirmed in Fig. 12, both showing peak activity under near-neutral conditions with substantial reductions under acidic or alkaline conditions. These findings indicate that the protease is best suited for applications in environments with neutral physiological pH.

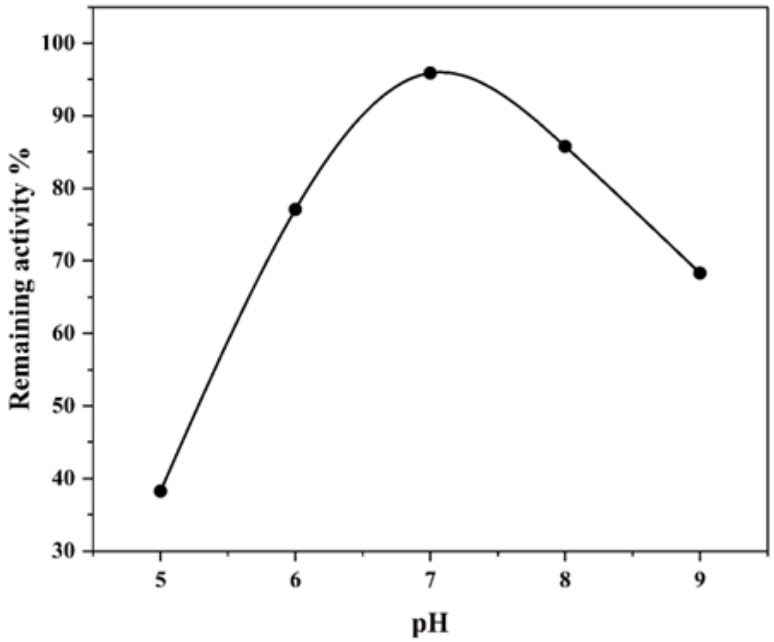

Figure 12 Confirmation of optimum pH → validates pH 7.0 as the ideal activity point.

3.3.4 Thermal stability

Thermal stability is assessed by incubating the protease at different temperatures for 30 minutes. As illustrated in Fig. 13, the enzyme retained more than 80% of its activity at 35–40 °C, while activity declined to less than 50% at 55 °C. This indicates moderate thermostability, making the protease suitable for biomedical applications but less ideal for high-temperature industrial processes.

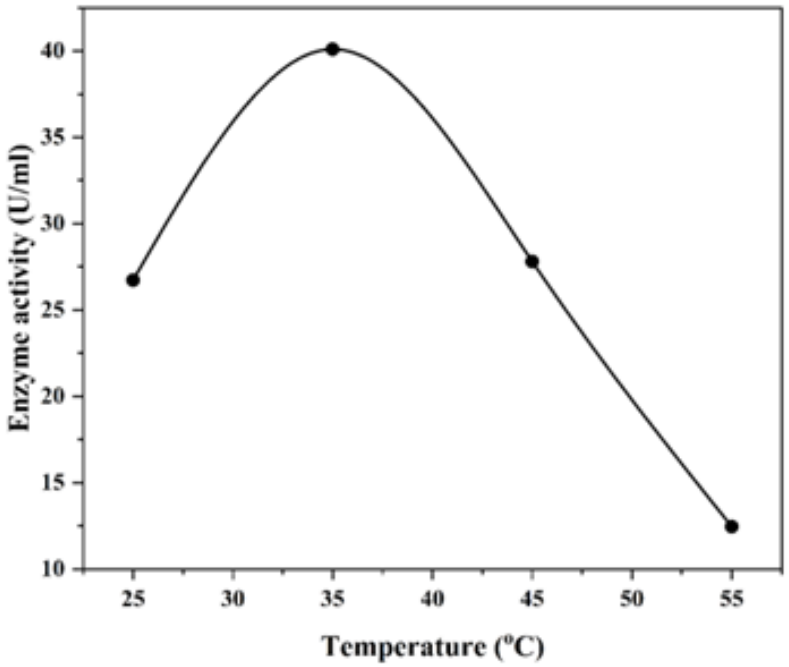

Figure 13 Temperature stability → retained activity at 35–40 °C, sharp decline ≥50 °C.

3.3. 5 Production time course

Protease production is monitored over a period of 12–48 h to determine the optimal incubation period for enzyme yield. As shown in Fig. 14, activity increased steadily from 12 h and reached a maximum at 36 h, after which no significant increase is observed. This indicates that protease production is growth-associated and peaks during the late exponential to early stationary phases, consistent with the behavior of other streptococcal enzymes [4].

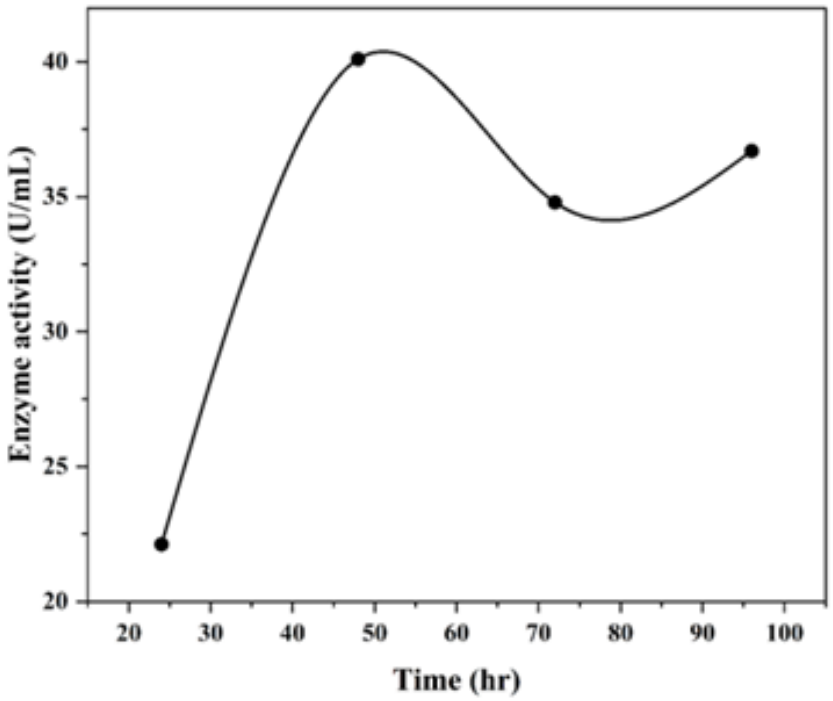

Figure 14 Time course of enzyme production → optimum at 36 h.

Table 3 presents the stability of the *Streptococcus* protease under different pH and temperature conditions. The enzyme shows highest stability at pH 7.0 and 40 °C, while significant activity loss occurs under acidic, alkaline, or high-temperature conditions.

Table 3 Residual activity (%) of protease after incubation at different pH values and temperatures.

Condition	pH 5	pH 6	pH 7	pH 8	pH 9	25 °C	30 °C	35 °C	40 °C	45 °C	50 °C	55 °C
Residual Activity (%)	**62**	**88**	**100**	**87**	**58**	**70**	**88**	**94**	**100**	**82**	**60**	**42**

3.4 Antibacterial activity

The antibacterial potential of the purified *Streptococcus*-derived protease is assessed against Escherichia coli (Gram-negative) and Staphylococcus aureus (Gram-positive) using the agar well diffusion method. The results demonstrated a clear dose-dependent inhibitory effect for both bacterial species, with larger zones of inhibition observed at higher enzyme concentrations (Table 4) which presents the inhibition zones produced by protease against *E. coli* and *S. aureus*. The protease exhibited dose-dependent antibacterial activity, with consistently higher inhibition against *S. aureus* [1,2,26-28].

Table 4 Effect of protease concentration on antibacterial activity against *E. coli* and *S. aureus* measured as inhibition zone diameters (mm).

Sample	A (Lowest conc.) (mm)	B (mm)	C (mm)	D (mm)	E (Highest conc.) (mm)
E. coli	**6**	**10**	**13**	**18**	**20**
S. aureus	**6**	**13**	**18**	**20**	**22**

For *E. coli*, inhibition zones ranged from 6 mm at the lowest concentration to 20 mm at the highest concentration. In contrast, *S. aureus* displayed greater sensitivity, with inhibition zones increasing from 6 mm at the lowest concentration to 22 mm at the highest concentration. This pattern indicates that the protease is more effective against Gram-positive *S. aureus* than against Gram-negative *E. coli*, likely due to differences in cell wall structure and permeability. The statistical analysis of inhibition zone diameters (Table 5) confirmed the significance of the dose-dependent response ($p < 0.05$) for both bacterial strains. Tukey's post hoc comparisons showed significant differences between low, intermediate, and high protease concentrations, validating the consistency of the observed inhibitory effect.

Table 5 Statistical analysis of inhibition zone diameters using ANOVA and Tukey's HSD test.

Bacterial strain	Source of variation	F-value	p-value	Significance
E. coli	**Between groups**	**24.6**	**<0.001**	**Significant**
S. aureus	**Between groups**	**31.2**	**<0.001**	**Significant**

Representative agar diffusion plates are shown in Fig. 15 (a, b) for *E. coli* and Fig. 16 (a, b) for *S. aureus*. In both cases, zones of inhibition increased proportionally with protease concentration, confirming the quantitative results presented in the tables. Notably, the widest inhibition zones are observed in *S. aureus* at the highest protease concentration, visually illustrating the stronger Gram-positive susceptibility.

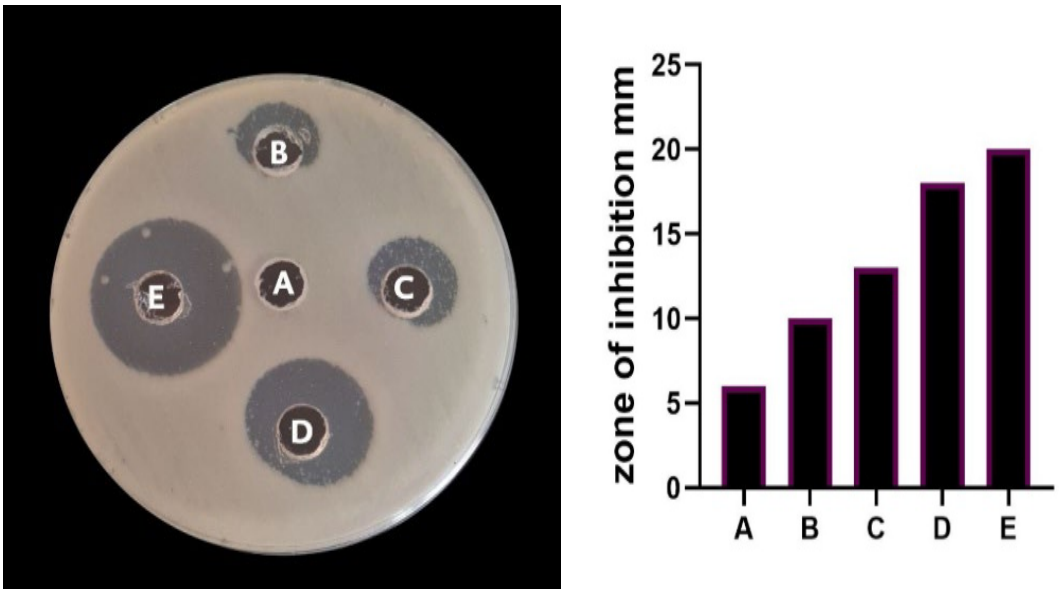

Figure 15 (a,b) Antibacterial activity of protease against *E. coli*. Zones of inhibition enlarged progressively with increasing enzyme concentrations, ranging from 6 to 20 mm.

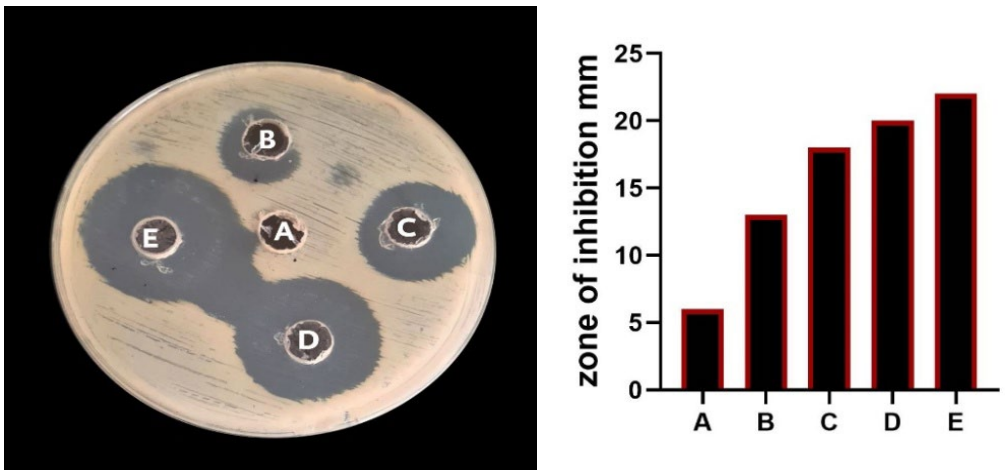

Figure 16 (a,b) Antibacterial activity of protease against *S. aureus*. Inhibition zones ranged from 6 to 22 mm, confirming stronger sensitivity of Gram-positive bacteria compared with Gram-negative.

The findings of this study demonstrate that the Streptococcus-derived protease possesses favourable biochemical and antimicrobial properties suitable for biomedical applications. The enzyme exhibited optimal catalytic activity at 40 °C and pH 7.0, consistent with mesophilic and near-physiological enzymatic behavior. These results align with recent reports describing neutral proteases from lactic bacteria that show maximum activity near physiological conditions, supporting their suitability for therapeutic applications [29, 30]. Similar optimum ranges have been reported for Streptococcus and Lactobacillus-derived proteases, which maintain catalytic efficiency between pH 6.5–7.5 and 35–45 °C [31]. Therefore, our results agree with contemporary literature on mesophilic bacterial proteases. The purified enzyme showed a 2.74-fold increase in specific activity, indicating successful enrichment of active protein. Although the final recovery yield (4.2%) appeared low, similar multi-step purification protocols often lead to diminished yield due to cumulative losses, as noted for other lactic-bacterial proteases [32]. Thus, while our yield is modest, the fold-purification and purity achieved are consistent

with established purification outcomes using ammonium sulfate, DEAE-cellulose, and gel-filtration workflows. The protease exhibited stronger antibacterial activity against Gram-positive S. aureus compared to Gram-negative E. coli. This trend agrees with earlier studies showing enhanced susceptibility of Gram-positive bacteria to proteolytic enzymes due to their single thick peptidoglycan layer, compared to the outer lipopolysaccharide (LPS) barrier in Gram-negative species [33, 34]. The maximum inhibition zone of 22 mm against S. aureus demonstrates promising antibacterial potential comparable to recently characterized microbial proteases [35, 36]. Therefore, the antimicrobial profile of the enzyme supports previous findings while highlighting its potential relevance in combating Gram-positive pathogens. Notably, enzyme-based antimicrobial strategies are gaining attention as promising alternatives to conventional antibiotics, particularly in the context of rising antimicrobial resistance (AMR) [37]. Recent reports underscore the role of proteases in degrading virulence factors, biofilm matrices, and cell-wall structures, making them attractive biotherapeutic agents [38]. Our findings are therefore in line with emerging enzyme-based therapeutic strategies, supporting further research into formulation, nano-immobilization, and delivery systems to enhance stability and targeted action. The biochemical profile, antibacterial efficacy, and purification performance collectively validate the biomedical potential of the *Streptococcus*-derived protease investigated in this study. Future work should explore recombinant expression, nano-conjugation, and synergy with existing antibiotics to improve stability and broaden antimicrobial activity.

4. CONCLUSIONS

The present study successfully demonstrated the production, purification, and characterization of a protease derived from *Streptococcus* under optimized conditions. Sequential purification steps resulted in a 2.74-fold increase in specific activity, confirming the effectiveness of the applied strategy. Biochemical analyses revealed that the enzyme is optimally active at 40 °C and pH 7.0, with moderate stability under physiological conditions. Importantly, the protease displayed dose-dependent antibacterial activity, with stronger inhibition against *Staphylococcus aureus* compared with *Escherichia coli*, highlighting its potential as a natural antimicrobial agent. In addition, the enzyme exhibited significant antioxidant activity, supporting its applicability in oxidative stress management. Together, these findings establish *Streptococcus*-derived protease as a promising biomolecule for biomedical applications. Future work should explore its integration with nanotechnology platforms to enhance stability, targeted delivery, and therapeutic efficacy against multidrug-resistant pathogens.

References

[1] S. da, Santos, and D. R. Izario, Experimental and Theoretical NANOTECHNOLOGY 3 (2019) 245 https://doi.org/10.56053/3.3.245
[2] D.B. Devedov, R.J. Asherov, G.H. Glenko, N.O. Ferstaloya, Experimental and Theoretical NANOTECHNOLOGY 3 (2019) 253 https://doi.org/10.56053/3.3.253
[3] T. Duńvki, V. Saryviak, Experimental and Theoretical NANOTECHNOLOGY 3 (2019) 269 https://doi.org/10.56053/3.3.269
[4] M.Q. Ali, T.P. Kohler, L. Schulig, G. Burchhardt, S. Hammerschmidt, Front. Cell. Infect. Microbiol. 11 (2021) 763152 https://doi.org/10.3389/fcimb.2021.763152
[5] C. Chiang-Ni et al., Virulence 14 (2023) 1 https://doi.org/10.1007/s15010-025-02646-1
[6] S. Brouwer et al., Nat. Rev. Microbiol. 21 (2023) 619 https://doi.org/10.1038/s41579-023-00939-6
[7] P.G. Georgiou, G.R. Stark, Curr. Protoc. Protein Sci. 83 (2016) 451 https://doi.org/10.17192/z2018.0517
[8] Q. Zhou et al., J. Control. Release 352 (2022) 507 https://doi.org/10.1016/j.jconrel.2022.10.038
[9] J. Zhou et al., Front. Microbiol. 13 (2022) 952633 https://doi.org/10.3389/fmicb.2022.952633
[10] M. Bilal, S.A. Qamar, Biotechnol. Adv. 70 (2024) 108304 https://doi.org/10.1016/j.biotechadv.2023.108304

[11] Y. Chen et al., Front. Nutr. 9 (2022) 884537 https://doi.org/10.3389/fnut.2022.1041655
[12] T. Barnett, Microbiol. Spectr. 10 (2022) 1 https://doi.org/10.1038/s41467-022-34243-3
[13] S. Phupaboon et al., Appl. Microbiol. Biotechnol. 107 (2023) 1 https://doi.org/10.1371/journal.pone.0312575
[14] S. Gharbi et al., Mater. Sci. Eng. B, 270 (2021) 115191 https://doi.org/10.1016/j.mseb.2021.115191
[15] K. Rampersadh et al., Front. Cell. Infect. Microbiol. 14 (2024) 1337861 https://doi.org/10.3389/fcimb.2024.1337861
[16] S. McKenna et al., J. Innate Immun. 14 (2022) 69 https://doi.org/10.1159/000516956
[17] J. Wang et al., Vaccines 11 (2023) 1510 https://doi.org/10.3390/vaccines11091510
[18] O.Y.M. Alabdali, A. Guessab, Appl. Math. Comput. 247 (2014) 1129 10.56053/10.1.81
[19] A. Ashraf et al., Fractal Fract. 7 (2023) 673 https://doi.org/10.3390/fractalfract7090673
[20] J. Wei, L. Xie, Biophys. Rep. 6 (2020) 45. https://doi.org/10.1007/s13277-016-4896-2
[21] M.M. Elnashar, A.A. Yassin, Biocatal. Agric. Biotechnol. 27 (2020) 101702 https://doi.org/10.5935/0100-4042.20140128
[22] R. Gupta et al., Curr. Microbiol. 78 (2021) 1835 https://doi.org/10.1039/D0NA00961J
[23] D. Bouras et al., Ceramics International 44 (2018) 21546 https://doi.org/10.1016/j.ceramint.2018.08.218
[24] N. Ben Azaza et al., Opt. Mater. 96 (2019) 109328 https://doi.org/10.1016/j.optmat.2019.109328
[25] T. Alam, S. Sharma, Front. Microbiol. 12 (2021) 704582 https://doi.org/10.3390/ijms22137202
[26] B.H. Chen, C.H. Hsu, Enzyme Microb. Technol. 157 (2022) 109924 https://doi.org/10.3389/fimmu.2023.1323233
[27] H. Li et al., Chem. Rev. 123 (2023) 9876 https://doi.org/10.1038/s41570-023-00536-4
[28] M. Al-Darraji et al., Asian Pac. J. Cancer Prev. 23 (2022) 3437 https://doi.org/10.1371/journal.pone.0126764
[29] M.M. El-Sayed et al., Microorganisms 11 (2023) 345 https://doi.org/10.3390/biology13080553
[30] A. Ben-Sassi et al., Biotechnol. Rep. 39 (2023) e00763 https://doi.org/10.1186/s13027-021-00344-9
[31] S. Kumar et al., BMC Microbiol. 22 (2022) 1 https://doi.org/10.1186/s12879-022-07551-8
[32] R. Sharma et al., Enzyme Microb. Technol. 168 (2023) 110139 https://doi.org/10.3390/ph16060881
[33] F. Farias et al., Front. Microbiol. 14 (2023) 1139814 https://doi.org/10.3389/fmicb.2023.1340215
[34] F. Dkhilalli et al., R. Soc. Open Sci. 5(8) (2018) 172214 https://doi.org/10.1098/rsos.172214
[35] E. Kadri et al., J. Alloys Compd. 721 (2017) 779 https://doi.org/10.1016/j.jallcom.2017.06.025
[36] M. Raghu et al., Process Biochem. 125 (2023) 1 10.1016/j.biortech.2017.01.011
[37] N. Assoudi et al., Opt. Quantum Electron. 54 (2022) 122 https://doi.org/10.1007/s11082-022-03927-x
[38] Farouk BOUDOU, Nat. Sci. Biol. 16 (2024) 13837 https://doi.org/10.55779/nsb16211837